Evaluating the Influence of Different Realistic Fibrosis Patterns on Cardiac Arrhythmias using Computational Models

Guilherme M Couto[1], Brodie A J Lawson[2], Kevin Burrage[2], Joventino O Campos[1], Rodrigo W dos Santos[1]

[1] Federal University of Juiz de Fora, Juiz de Fora, Brazil
[2] Queensland University of Technology, Brisbane, Australia

Abstract

Fibrosis disrupts cardiac conduction, increasing arrhythmia risk. Its morphology plays a key role in arrhythmogenicity. Using Perlin noise, we generated four fibrosis patterns — compact, diffuse, interstitial, and patchy — and assessed their impact on reentry dynamics via cardiac simulations. We determined the percolation threshold for each type and examined the effects of fiber orientation and density. Results showed that diffuse fibrosis is the most arrhythmogenic, while compact is the least. These insights refine computational models and advance the understanding of fibrosis-driven arrhythmogenesis.

1. Introduction

Cardiac fibrosis is a broad term referring to the excessive accumulation of extracellular matrix within heart tissue. It is well-established that it has a profound impact on both electrical propagation and the tissue's arrhythmogenic potential [1,2]. These collagen-rich scars act as barriers to the propagation of electrical signals, creating intricate regions that strongly promote the formation of spirals associated with arrhythmias. They can induce unidirectional blocks that give rise to reentry circuits, which surpass the refractory period of the cells.

Therefore, the architecture of this labyrinth, i.e., the morphology of these lesions, plays a pivotal role in determining the propagation pathway of electrical activity and, consequently, the likelihood of arrhythmia occurrence [3]. Histological studies of cardiac tissue have identified four primary types of fibrosis: *compact*, *diffuse*, *interstitial*, and *patchy* [1, 2]. Unfortunately, due to the limited resolution of imaging techniques, these microstructural variations are generally not taken into account in most current cardiac models. However, recent advancements make it possible to incorporate these histological features into simulations, enabling the generation of more realistic fibrosis patterns using Perlin noise fields [4]. They produce natural-looking patterns with controllable feature sizes by smoothly interpolating random gradient values across a grid. This approach allows the creation of complex, spatially coherent structures that resemble the microstructural variability observed in biological tissues.

2. Methods

Leveraging these computational tools, this paper explores the arrhythmogenic potential of different fibrosis patterns by integrating percolation theory and high-performance simulations. First, we identify the percolation threshold for each fibrosis type, and, based on it, we perform simulations to analyze how each structural pattern influences electrical propagation and the likelihood of sustained reentries.

2.1. Fibrosis model

In this paper, we used a generator based on Perlin noise to create realistic fibrosis patterns that closely mimic the medical literature classification. Interstitial fibrosis is characterized by collagen accumulation between cardiomyocyte clusters, forming a fine mesh. Compact fibrosis consists of dense, contiguous fibrotic regions entirely devoid of myocardial cells. Diffuse fibrosis manifests as short, scattered collagen segments interspersed within the myocardium. Patchy fibrosis, on the other hand, features long, irregular collagen strands interwoven with myocardial bundles [1, 2]. As shown in Figure 1, the method successfully reproduced these key morphological features.

Owing to the stochastic nature of noise field generation, a single set of parameters can yield distinct patterns while preserving the defining anatomical characteristics of each classification. To assess the arrhythmogenic potential of these fibrotic structures, we adopted the same parameter set as Lawson et al. [4], except for fiber orientation and fibrosis density within the mesh.

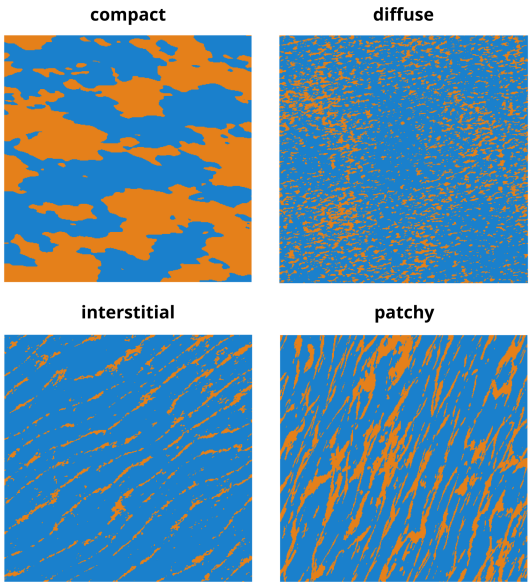


Figure 1. Representative examples of the four primary fibrosis patterns, computationally generated from predefined parameters using Perlin noise. Blue regions denote healthy tissue, while orange regions denote fibrotic tissue.

2.2. Percolation threshold

Reentries tend to occur within a range of densities that is close to the percolation threshold [5], defined as the critical fibrosis density where 50% of the tested samples exhibit conduction across the domain and 50% do not. To estimate this threshold, we used a 4 cm × 4 cm domain and tested all four fibrosis patterns at orientations from 0° up to 90° with increments of 30°.

For each combination of pattern, density, and orientation, 100 independent samples were generated. A Python script based on cellular automata was then used to determine the proportion of samples in which an unbroken path connected the left and right sides of the domain.

In this approach, the domain was discretized into a grid of square automata, each 100 μm in size. Each automaton directly corresponded to a single pixel in the synthetic fibrosis maps generated by the Perlin noise algorithm, meaning each pixel was interpreted as either filled (fibrotic) or empty (healthy), based on the underlying pattern.

Initially, all elements in the leftmost column were set to an active state, representing an external electrical stimulus. During each iteration, an automaton became active if at least one of its neighboring elements (above, below, left, or right) had already been activated in the previous step. Fibrotic automata could not be activated, effectively preventing conduction through these areas.

The process concluded under one of two conditions: (i) if any automaton in the last column on the right became active, confirming the presence of a continuous conduction path, or (ii) if no further activations occurred, indicating that all possible pathways had been exhausted.

2.3. Mathematical model

To mathematically model the propagation of electrical excitation through cardiac tissue, we adopted the monodomain reaction-diffusion equation, as [5]. The conductivity tensor, $\boldsymbol{\sigma}$, accounts for tissue anisotropy, with a longitudinal component of $\sigma_l = 1.334 \times 10^{-4}$ mSμm^{-1} and an intra-transverse component of $\sigma_n = 1.76 \times 10^{-5}$ mSμm^{-1}. To complete the formulation, the model was subject to appropriate initial conditions and incorporated no-flux boundary constraints, ensuring that the tissue periphery remained electrically isolated.

Coupled with the monodomain model, we adopted a modified version of the ten Tusscher (TT3) cellular model [6] to represent epicardial cells in the human ventricular wall. Given that fibrosis and ischemia are frequently coexisting conditions in cardiac pathology, we introduced adaptations to account for the electrophysiological effects of hypoxia, modeled as a reduction in intracellular adenosine triphosphate (ATP) levels. Specifically, an outward potassium current, $I_{K(ATP)}$, was incorporated into the model, as its activation is sensitive to ATP depletion. Additionally, the conductance of the L-type calcium current, I_{CaL}, was adjusted to depend on ATP availability. In this study, the intracellular ATP concentration, $[\text{ATP}]_i$, was set to 2 mM, representing an acute ischemic condition, as the physiological baseline is typically 5.4 mM. This ischemic behavior has been previously modeled [5].

2.4. Computational simulations

The computational domain was considered fully injured and measured 4 cm × 4 cm × 100 μm, with cubic volumes of 100 μm per side and a temporal discretization of 0.02 ms. In the experiments, a single external stimulus was applied for 2 ms along the entire left boundary of the mesh, spanning the full vertical extent and reaching up to 500 μm along the horizontal axis. To account for the stochastic nature of fibrosis distribution, a Monte Carlo approach was employed, generating 100 different samples for each fibrosis proportion. Densities ranged from 0.05 to 0.7 in increments of 0.05, as percolation analysis indicated that testing densities above 0.7 was unnecessary (see Table 1). Reentry was classified as sustained if active cells were still present at the end of the 1000 ms simulation.

Simulations were performed using the high-performance solver MonoAlg3D, which leverages GPUs to accelerate computation [7]. The partial differential equation was solved with the finite volume method, while the ordinary

differential equations governing cellular dynamics were integrated using the Rush-Larsen scheme.

3. Results and discussions

The percolation thresholds detailed in Table 1 were fundamental to strategically refining the scope of our arrhythmogenicity assessment. The analysis revealed that the highest threshold for electrical disconnection across all configurations was 64%. Since sustainable re-entrant circuits are known to form primarily in regimes below this critical point [5], this result provided a clear and robust justification for setting a 70% fibrosis density as the upper limit for our electrophysiological simulations. This approach concentrated our efforts on the most pro-arrhythmic conditions, thereby ensuring the integrity of the findings while improving the computational efficiency.

The analysis of Table 1 also sheds light on interesting anisotropic behaviors. For instance, the elongated structure of interstitial and patchy fibrosis explains their lower percolation thresholds in the transverse direction (90°) when compared to the longitudinal one (0°).

Table 1. Percolation thresholds expressed as fibrosis densities for different fibrosis types and fiber orientations.

Fibrosis Type	0°	30°	60°	90°	Avg
Compact	0.64	0.56	0.41	0.34	0.49
Diffuse	0.50	0.48	0.47	0.47	0.37
Interstitial	0.52	0.48	0.41	0.38	0.45
Patchy	0.53	0.47	0.35	0.31	0.41

Figure 2 presents the relationship between fibrosis density (x-axis) and the percentage of sustained reentries (y-axis), revealing key insights into the arrhythmogenic behavior of different fibrosis patterns. The curves were fitted using the Piecewise Cubic Hermite Interpolating Polynomial method available in the SciPy library.

Figure 2 highlights the distinct influence of fiber orientation. A reduction in arrhythmogenesis was observed at oblique angles (30° and 60°), a behavior likely attributable to the staircase effect inherent to the cubic finite volume discretization, which reduces the occurrence of unidirectional blocks. However, at grid-aligned orientations (0° and 90°), fibrosis types behaved differently. Diffuse fibrosis peaked at 0°, suggesting a severe disruption of longitudinal propagation. In contrast, interstitial and patchy patterns were more arrhythmogenic at 90°, likely because their elongated strands, when aligned perpendicularly to the stimulus, act as more effective barriers to conduction.

Among the four patterns, compact fibrosis was the least arrhythmogenic, as anticipated [1, 3]. Patchy fibrosis followed a similar trend but with slightly higher susceptibility, reinforcing the observation that clustered fibrotic regions are less prone to generating reentries than dispersed ones. Conversely, diffuse fibrosis was the most consistently arrhythmogenic pattern, followed by the interstitial pattern. These results indicate that small, scattered obstacles are significantly more efficient at promoting unidirectional blocks and sustaining reentry than larger aggregated cores, as found in [3].

To further illustrate the distinct mechanisms underlying reentry formation in different fibrosis patterns, Figure 3 presents frames of a reentrant circuit for each fibrosis type. In the cases of compact and diffuse fibrosis, the reentrant wavefronts exhibited a predominantly circular propagation. For compact fibrosis, the reentry was sustained because the large fibrotic core provided a sufficiently wide path for the excitation wave to circulate. Circular patterns were also observed in diffuse fibrosis. This specific pattern is more likely to generate regions with microstructures that exhibit a source-sink mismatch, the fundamental mechanism underlying unidirectional block and reentry as observed in our experiments.

For interstitial and patchy fibrosis, the reentry pathways exhibited a more zig-zag conduction pattern instead of a circular one. This behavior was a direct consequence of their elongated fibrotic structures aligned with the direction of the fibers. These structural characteristics forced the excitation wave to propagate through tortuous routes, further sustained by unidirectional conduction blocks that promoted reentry formation. This irregular conduction pattern is particularly relevant in understanding how structural heterogeneity influences arrhythmogenesis.

4. Conclusions

This study provides new insights into the arrhythmogenic effects of different fibrosis morphologies using a combination of percolation theory and computational simulations. We demonstrated that the spatial distribution of fibrosis, particularly its alignment relative to the propagation of electrical waves, has a profound impact on reentry formation. Our findings suggest that the probability of reentry in interstitial and patchy fibrosis, due to their elongated structures, exhibits high sensitivity to the angle between the fibers and the propagating wave-front, whereas diffuse fibrosis was consistently the most arrhythmogenic pattern. These results emphasize the importance of incorporating realistic fibrosis patterns into computational cardiac models to improve their predictive power.

While this study provides valuable insights, it was limited to two-dimensional domains, a single parameter set, and a fully fibrotic and ischemic scenario. Future work will address these limitations by extending the analysis to three-dimensional domains and heterogeneous conditions, which are critical to capture more realistic dynam-

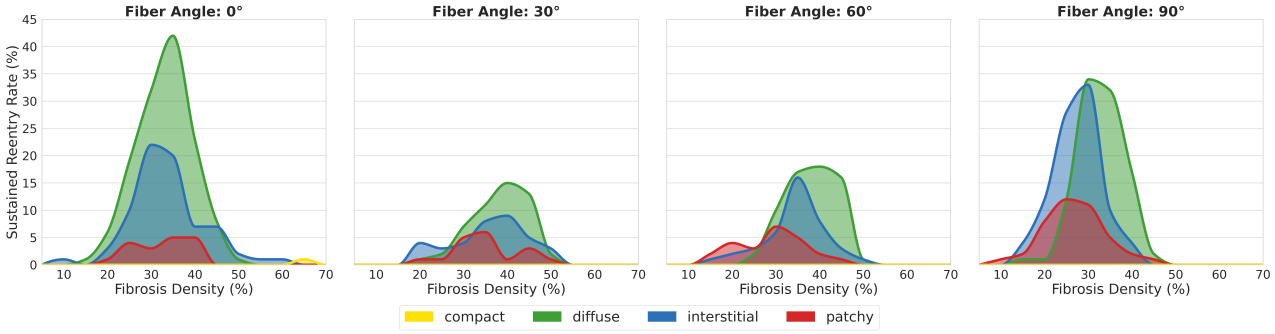


Figure 2. Relationship between fibrosis density and the percentage of sustained reentries for different fibrosis types and fiber orientations. The figure consists of four subplots corresponding to fiber orientations of 0°, 30°, 60°, and 90°. Different fibrosis patterns are color-coded: yellow for compact, green for diffuse, blue for interstitial, and red for patchy.

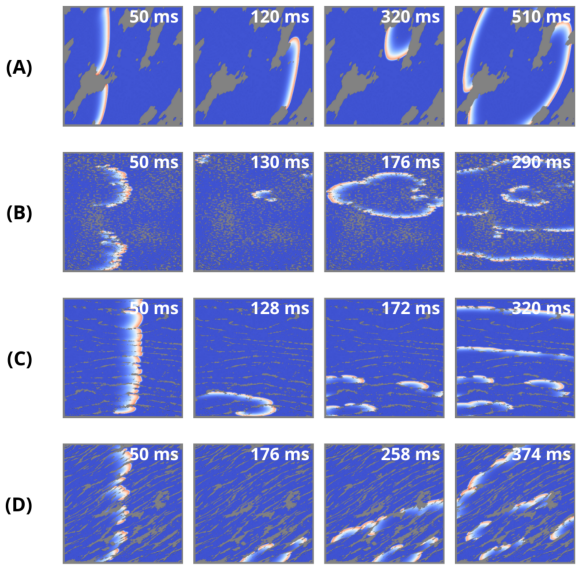


Figure 3. Time evolution of a reentrant circuit for different fibrosis patterns. Each subfigure (A–D) presents four time frames illustrating the evolution of the reentrant waves. (A) Compact, (B) Diffuse, (C) Interstitial and (D) Patchy.

ics. In addition, as the present work focused on ventricular ionic models, future investigations will also explore atrial models to better understand fibrosis-driven mechanisms in atrial fibrillation.

Acknowledgments

The authors acknowledge support from the Wellcome Trust (214290/Z/18/Z), EPSRC via the CompBioMedX project (EP/X019446/1), CompBioMed2 (GA 675451, 823712), FAPEMIG (PCE-00048-25; APQ-02752-24; APQ-02445-24; APQ-02513-22), FINEP (SOS Equipamentos AV020062/22), SINAPAD Santos-Dumont, CAPES, EBSERH, and UFJF.

References

[1] De Jong S, van Veen TA, van Rijen HV, de Bakker JM. Fibrosis and cardiac arrhythmias. Journal of Cardiovascular Pharmacology 2011;57(6):630–638.

[2] Hinderer S, Schenke-Layland K. Cardiac fibrosis–a short review of causes and therapeutic strategies. Advanced Drug Delivery Reviews 2019;146:77–82.

[3] Mulimani MK, Lawson BA, Pandit R. Arrhythmogenicity of cardiac fibrosis: fractal measures and betti numbers. arXiv preprint arXiv210500181 2021;.

[4] Lawson BA, Drovandi C, Burrage P, Bueno-Orovio A, Dos Santos RW, Rodriguez B, Mengersen K, Burrage K. Perlin noise generation of physiologically realistic cardiac fibrosis. Medical Image Analysis 2024;98:103240.

[5] Sachetto R, Alonso S, Dos Santos RW. Killing many birds with two stones: hypoxia and fibrosis can generate ectopic beats in a human ventricular model. Frontiers in Physiology 2018;9:764.

[6] Ten Tusscher KH, Panfilov AV. Cell model for efficient simulation of wave propagation in human ventricular tissue under normal and pathological conditions. Physics in Medicine Biology 2006;51(23):6141.

[7] Sachetto Oliveira R, Martins Rocha B, Burgarelli D, Meira Jr W, Constantinides C, Weber dos Santos R. Performance evaluation of gpu parallelization, space-time adaptive algorithms, and their combination for simulating cardiac electrophysiology. International Journal for Numerical Methods in Biomedical Engineering 2018;34(2):e2913.

Address for correspondence:

Guilherme Martins Couto
Programa de Pós-Graduação em Modelagem Computacional (PPGMC-UFJF) - Juiz de Fora - MG, Brasil, 36036-330
guilherme.couto@estudante.ufjf.br